Synthesis and Characterization of Polypyrrole Dodecylbenzenesulfonate-Titanium Dioxide Nanocomposites

Abdul Shakoor, Tasneem Zahra Rizvi

Department of Physics, Quaid-i-Azam University, Islamabad 45320, Pakistan

Received 4 January 2009; accepted 21 September 2009
DOI 10.1002/app.31512
Published online 26 March 2010 in Wiley InterScience (www.interscience.wiley.com).

ABSTRACT: Nanocomposites of polypyrrole dodecylbenzenesulfonate-titanium dioxide have been prepared from a colloidal solution of titanium dioxide (TiO_2) nanoparticles. The DC conductivity of samples with different concentrations of TiO_2 has been investigated under dark and light. The doping effect of TiO_2 has been characterized and evaluated by transmission electron microscopy (TEM), Fourier transform infrared spectroscopy, and X-ray diffraction. TEM shows that TiO_2 nanoparticles have strong effects on the morphology of composites, and conductivity measurements show that the conductivity first increases and then decreases as the percentage of TiO_2 is increased in the composites exhibiting a maximum in conductivity at about 20 wt % of TiO_2. © 2010 Wiley Periodicals, Inc. J Appl Polym Sci 117: 970–973, 2010

Key words: PPy.DBSA; TiO_2; conductivity; photoconductor

INTRODUCTION

Polypyrrole (PPy) has drawn a lot of interests because of thermal and atmospheric stability,[1,2] poor solubility in common solvent, however, made PPy's practical applications limited in many areas.[3,4] Jang et al.,[5] Campos et al.,[6] and Aleshin et al.[7] reported soluble PPy by polymerizing pyrrole monomer in the presence of dodecylbenzenesulfonate (DBSA). The application of soluble PPy-DBSA is in the fabrication of Schottky diodes and in organic field effect transistors (OFETs).[6,8,9]

The combination of conducting polymers with nanoparticles, such as MnO_2,[10] TiO_2,[11] Y_2O_3,[12] $CdPS_3$,[13] V_2O_5,[8] Mo O_3,[14] and FeOCl,[15] is an important alternative to obtain new polymeric materials with designed properties. In such nanocomposites, the insulating nanoparticles provide good mechanical properties and thermal stability while the conducting polymer would provide electrical conductivity. Further, there is an increasing demand for polymeric materials whose electrical conductivity can be tailored for a given application, and that have attractive combined mechanical and other properties. Thus, this have been the driving force for many of the researches in conductive blends to obtain a wide range of conductivity, which is controllable with varied weight fraction of the conducting polymer for various potential applications.[16,17]

EXPERIMENTAL

Chemicals and materials

Pyrrole was obtained from ALDRICH and vacuum distilled before use. Ammonium per sulfate (APS) was obtained from FLUKA, and TiO_2 was supplied by Aldrich and used as obtained.

Synthesis of PPY-DBSA

A total of 0.15 mol of DBSA was dissolved in 100 mL distilled water, then 0.03 mol of pyrrole was added, and the solution was kept on magnetic stirring. After 3 h, 0.15 mol of the oxidant APS dissolved in 200 mL distilled water was added dropwise under vigorous stirring. After 24 h, 1 L methanol was added in the solution and was kept at room temperature (25°C). After 2 days, the suspension was filtered and washed. The black paste of PPy.DBSA was obtained, which was dried under vacuum at 70°C for 24 h.

Synthesis of PPY-DBSA TiO_2 nanocomposites

An appropriate amount of TiO_2 was suspended in chloroform. After 2-h sonication, the required amount of PPy-DBSA was added in the suspension. The composites were finally dried under vacuum for 48 h at 40°C. The different PPy.DBSA-TiO_2 composites were synthesized using 1.0, 5, 10.15, 20, 25, 30,

Correspondence to: A. Shakoor (shakoor_47@yahoo.com).
Contract grant sponsors: Higher Education Commission (HEC), Pakistan, International Research Support initiative Program (IRSIP).

35, 40, 45, and 50 wt % of TiO_2 with respect to PPy-DBSA.

Measurement

The pellets for conductivity measurements were made in SPECAC KBr press under vacuum at 10 ton pressure in 13-mm diameter stainless steel die. Electrical conductivity measurements were performed using the Van der Pauw four-probe technique.

The samples were connected to a Keithley617 programmable electrometer and Keithley 224 programmable current source under computer control. The conductivity and reproducibility of all the samples were checked. X-ray diffraction (XRD) analysis was carried out using an automated diffractometer, Bruker-AXS model D8, using Cu Kα radiations. The instrument was operated at 40 KV and 30 mA, and the diffraction patterns of PPy.DBSA-TiO_2 nanocomposites samples mounted on a standard holder were recorded over the range of 8°–60°; counting time was 3 s and the step size was 0.10. The Fourier transform infrared spectra were recorded on KBr pellet samples in the range of 4000–400 cm^{-1} using a Perkin-Elmer Fourier transform infrared spectrometer. The thermogravimetric analysis (TGA) was carried out on Mettler thermobalance STAR S.W. 8.10 from room temperature (25°C) to 700°C for all the samples. The samples were heated at the rate of 10°C/min in nitrogen atmosphere. Transmission electron microscopy (TEM) was carried out on an EVO50 ZEISS instrument, and the samples were prepared by microtoming.

RESULTS AND DISCUSSION

Figure 1 shows the typical micrographs of pure TiO_2 nanoparticles and PPy.DBSA-TiO_2 composite. It could be seen that the pure TiO_2 nanoparticles were spherical in shape with the size in the range of 30–40 nm (Fig. 1), and the PPy.DBSA-TiO_2 composite was spherical and the diameters were in the range of 30–40 nm (Fig. 1).

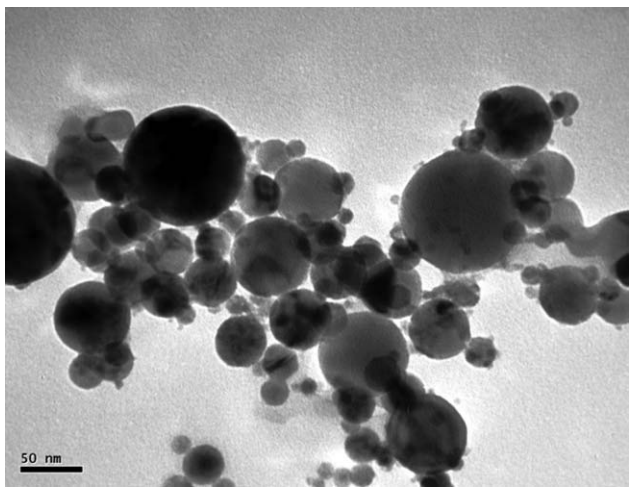

Figure 1 TEM images of PPy.DBSA-TiO_2 nanocomposites.

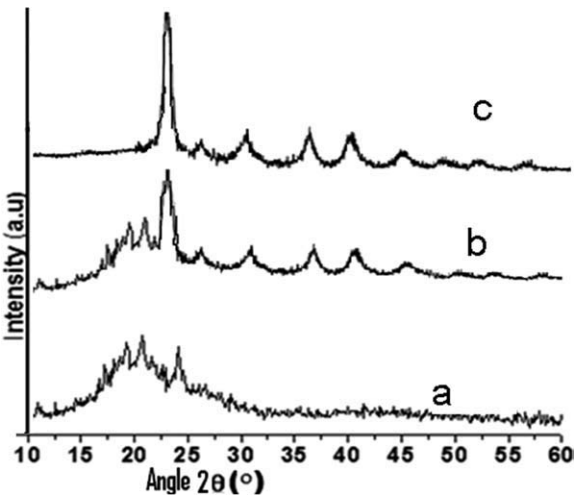

Figure 2 The XRD patterns of (a) PPy.DBSA, (b) PPy.DBSA-TiO_2 nanocomposites, and (c) TiO_2 pure.

Figure 2 presents the XRD patterns of TiO_2 nanoparticles, PPy.DBSA, and PPy.DBSA-TiO_2 composite. It is apparent that the obtained TiO_2 nanoparticles are crystalline, and all the peaks reveal that the TiO_2 is rutile phase. Adopting the Scherrer formula, the calculated size of TiO_2 particles is 30.4 nm, consistent with the observed result of TEM (Fig. 1). Figure 2(a) indicates that PPy.DBSA is also semicrystalline. Along with broad peak, five diffraction peaks in the region of $2\grave{e} = 10°–30°$ can be observed, and two relatively strong peaks, centered at 20.81° and 24.93°, should be ascribed to the periodicity parallel and perpendicular to the PPy.DBSA-conjugated chain, respectively. The XRD pattern of PPy.DBSA-TiO_2 composite shows the characteristic peaks not only for the PPy.DBSA but also for the TiO_2 nanoparticles [Fig. 2(b)]. It was confirmed that the nanocomposites are composed of PPy.DBSA and TiO_2 nanoparticles.

Figure 3 shows the FTIR spectra of PPy.DBSA and PPy.DBSA-TiO_2 nanocomposites. The main characteristic bands of PPy.DBSA were assigned as follows:

A band at 3410 cm^{-1} attributed to N—H stretching. The absorption band in region 1200 cm^{-1} N—H in the plane mode, and it was characteristic band for PPy. The band at 1090 cm^{-1} corresponds to symmetric C—H in the plane mode. The stretching modes of polypyrrole are shown in the region 1600–1400 cm^{-1}. The absorption observed at 1550 cm^{-1} corresponds to C—C stretching mode of PPy chains[8] is also characteristics bands of this material. The C=C stretching vibrations at 1560 and 1480 cm^{-1}, C—N,

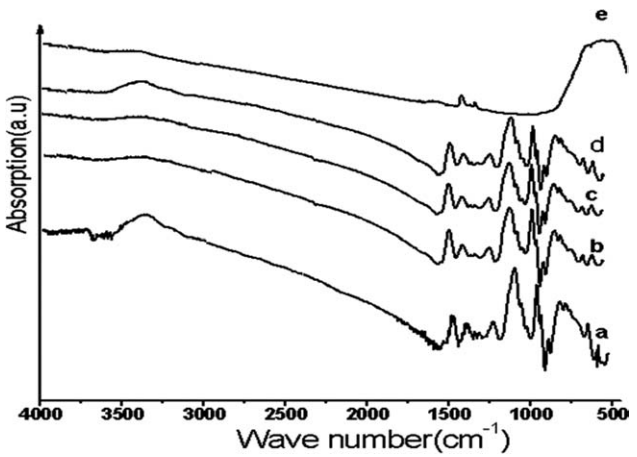

Figure 3 FTIR spectra of (a) PPy.DBSA, (b) 1%, (c) 5%, (d) 10% TiO_2 in PPy.DBSA-TiO_2 nanocomposites, and (e) TiO_2 pure.

C—C vibrations at 1394 cm^{-1}, C—H out-of-plane bending vibration of PPy of polymer chain and C—H in plane bending vibration of 110 cm^{-1}, and C—H out-of-plane bending vibration of 933 cm^{-1} are proposed to form the PPy polymer main chains.[18,19]

The spectrum of PPy.DBSA-TiO_2 composite shows that all the characteristic bands of PPy.DBSA appeared and obviously shifted to the lower wavenumbers, but the characteristic bands of TiO_2 nanoparticles did not appear from which it was recognized that a strong interaction exists between PPy.DBSA and TiO_2 nanoparticles.

The electrical conductivity of the pressed pellets PPy.DBSA-TiO_2 nanocomposites is measured by the four-probe technique under dark and light. All the pellets show high conductivity, probably because the well-extended conjugation conformation of the doped PPy is retained. Figure 4 shows the conductivity of PPy.DBSA-TiO_2 composite at different contents of TiO_2 and the effect of light. The conductivity of the nanocomposites increases slightly with increasing TiO_2 content and then decreases with excess TiO_2 content. Similar phenomenon was also found for the nanocomposites of PAni.DBSA-TiO_2.[20] It is because of the fact that TiO_2 is a photoconductor and the conductivity enhanced under light when compared with darkness. The increase in conductivity with TiO_2 contents could be attributed due to alignment and straightening of PPy.DBSA chains on the surface of TiO_2 nanoparticles. At 20% of TiO_2, this alignment and straightening of chains of the polymers become maximum, and as we add more TiO_2 the conductivity decreases due to insulating behavior of TiO_2. When the quantity of TiO_2 is less than 20 wt %, the insulating behavior is not dominant and conductivity increases due to straightening of PPy.DBSA chains. When the TiO_2 contents increases from 20%, the increase in conductivity due to straightening of PPy.DBSA chains is not dominant and insulating behavior of TiO_2 became dominant and conductivity is decreased

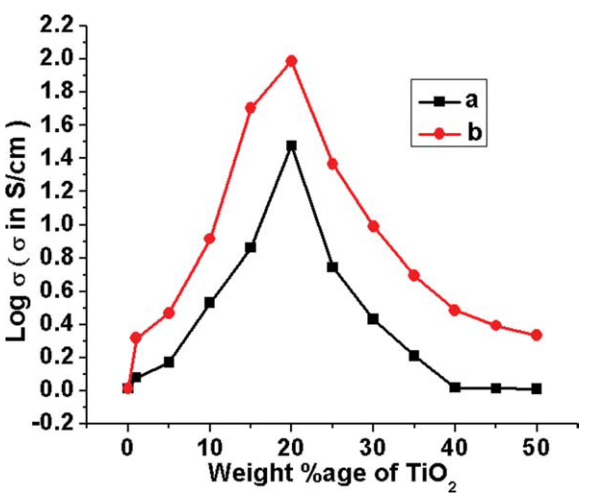

Figure 4 Graph of log σ versus wt % of TiO_2 in PPy.DBSA-TiO_2 (a) in dark and (b) in light. [Color figure can be viewed in the online issue, which is available at www.interscience.wiley.com.]

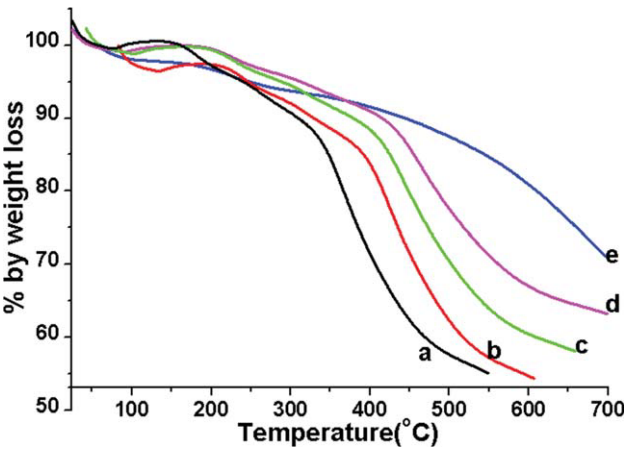

Figure 5 TGA of (a) PPy.DBSA, (b) 5%, (c) 15%, (d) 20%, and (e) 30% TiO_2 in PPy.DBSA-TiO_2 nanocomposites. [Color figure can be viewed in the online issue, which is available at www.interscience.wiley.com.]

PPy.DBSA-TiO_2 nanocomposites were investigated by TGA as shown in Figure 5. It can be easily seen that the thermal stability of PPy.DBSA-TiO_2 composites is much higher than that of the doped polymer because of its conjugated stiff backbone on nanoparticles of TiO_2. Hence, the thermal stability of the nanocomposites increases with the increase of TiO_2.

CONCLUSIONS

We developed new process for the preparation of conducting PPy.DBSA-TiO_2 nanocomposites. Conductivity of doped PPy increases with the increase of TiO_2 contents up to 20% by weight and then

decreases, and the conductivity was affected by light, the chains of PPy.DBSA are aligned and straightened due to which conductivity increases. This alignment is maximized up to 20 wt % of TiO_2 in PPy.DBSA, that is why conductivity increases up to this level and then decreases due to insulating behavior of TiO_2. Such processable nanocomposites will be promising candidates for advanced materials to be used in the high-technology industries in the future, and work on the exploration of its applications is currently underway. Thermal stability was found to be enhanced by adding TiO_2 nanoparticles in PPy.DBSA-TiO_2 nanocomposites.

The authors are grateful to Prof. Dr. P. J. S., Foot Materials Research Group, Kingston University, London, for extending his laboratory facilities. They are also grateful to Dr. Simon De Mars for running the thermal analysis and Richard Digen for running SEM.

References

1. Salmon, M.; Kanazawa, K. K.; Diaz, A. F.; Krounby, M. J Polym Sci Polym Lett Ed 1982, 20, 187.
2. Chen, S. A.; Liao, C. S. Macromolecules 1993, 26, 2810.
3. Chao, S.; Wrighton, M. S. J Chem Soc 1987, 109, 2197.
4. Merz, M.; Haimerl, A.; Owen, A. J. Synth Met 1988, 25, 89.
5. Jang, K. S.; Lee, H.; Moon, B. Synth Met 2004, 143, 289.
6. Campos, M.; Simoes, F. R.; Pereira, E. C. Sens Actuators B 2007, 125, 158.
7. Aleshin, A. N.; Lee, K.; Lee, J. Y.; Kim, D. Y.; Kim, C. Y. Synth Met 1999, 99, 27.
8. Loi, Y. J.; Degrott, D. C.; Schindler, J. L.; Kannewurf, C. R.; Kanatzidis, M. G. Adv Mater 1993, 5, 369.
9. Shakoor, A.; Rizvi, T. Z.; Nasir, M.; Sulaman, M.; Ishtiaq, M. J Mater Electron, to appear; DOI:10, 1007/s10854-009-9964-6.
10. Gemeay, A. H.; Mansour, I. A.; El-Sharkawy, R. G.; Zaki, A. B. Eur Polym J 2005, 41, 2575.
11. Bitao, S. U.; Shixiong, M.; Shixiong, S.; Yongchun, T.; Jie, B. Front Chem China 2007, 2, 123; DOI 10.1007/s11458-007-0025-5.
12. Vishnuvardhan, T. K.; Kulkarni, V. R.; Basavaraja, C.; Raghavendra, S. C. Bull Mater Sci 2006, 29, 77.
13. Clemmet, R.; Green, M. L. H. J Chem Soc Dalton Trans 1979, 21, 1566.
14. Hill, P. G.; Foot, P. J. S.; Davis, R. Synth Met 1996, 76, 289.
15. Hill, P. G.; Foot, P. J. S.; Budd, D.; Davis, R. Mater Sci Forum 1993, 122, 185.
16. Omastova, M.; Kosina, S.; Pionteck, J.; Janke, A.; Pavlinec, J. Synth Met 1996, 81, 49.
17. Ikkala, O. T.; Laakso, J.; Vakiparta, K.; Virtanen, E.; Ruohonen, H.; Jarvinen, H.; Taka, T.; Passiniemi, P. Synth Met 1995, 69, 97.
18. Jang, K. S.; Lee, H.; Moon, B.; Kim, C. Y. Synth Met 2004, 143, 289.
19. Lamprakopoulos, S.; Yfantis, D.; Yfantis, A.; Schmeisser, D. Synth Met 2004, 144, 229.
20. Su, S.-J.; Kuramoto, N. Synth Met 2000, 114, 147.